

Geophysical Research Letters

RESEARCH LETTER

10.1029/2018GL079061

Key Points:

- The ca. 21 Ma mafic enclaves in southern Tibet originated from the primary ultrapotassic magmas
- The primary ultrapotassic magmas were derived from a mantle source metasomatized by the subducted Indian continent
- The Indian continent had subducted beneath central Lhasa no later than the early Miocene

Supporting Information:

- Supporting Information S1

Correspondence to:

Q. Wang,
wqiang@gig.ac.cn

Citation:

Hao, L.-L., Wang, Q., Wyman, D. A., Qi, Y., Ma, L., Huang, F., et al. (2018). First identification of mafic igneous enclaves in Miocene lavas of southern Tibet with implications for Indian continental subduction. *Geophysical Research Letters*, 45, 8205–8213. <https://doi.org/10.1029/2018GL079061>

Received 2 JUN 2018

Accepted 2 AUG 2018

Accepted article online 13 AUG 2018

Published online 22 AUG 2018

First Identification of Mafic Igneous Enclaves in Miocene Lavas of Southern Tibet With Implications for Indian Continental Subduction

Lu-Lu Hao^{1,2} , Qiang Wang^{1,3,4} , Derek A. Wyman⁵ , Yue Qi¹, Lin Ma¹, Fang Huang² , Le Zhang¹, Xiao Ping Xia¹ , and Quan Ou¹

¹State Key Laboratory of Isotope Geochemistry, Guangzhou Institute of Geochemistry, Chinese Academy of Sciences, Guangzhou, China, ²CAS Key Laboratory of Crust-Mantle Materials and Environments, School of Earth and Space Sciences, University of Science and Technology of China, Hefei, China, ³CAS Center for Excellence in Tibetan Plateau Earth Sciences, Beijing, China, ⁴College of Earth and Planetary Sciences, University of Chinese Academy of Sciences, Beijing, China, ⁵School of Geosciences, The University of Sydney, Sydney, New South Wales, Australia

Abstract The history of Indian continental subduction beneath Asian plate remains unclear. Miocene ultrapotassic rocks in southern Tibet, with extremely enriched isotopes, have often been used to trace mantle metasomatism and geodynamic processes associated with Indian continental subduction. These rocks, however, may have been contaminated by Lhasa ancient crust. Uncertainties on primary ultrapotassic magmas obscure their mantle sources. Here we report on first mafic igneous enclaves in Cenozoic lavas of southern Tibet. They consist principally of clinopyroxene, phlogopite, and sanidine and have a zircon U-Pb age of 21.5 ± 0.3 Ma. Mineral and bulk-rock geochemical characteristics indicate their crystallization from primary ultrapotassic magmas. Bulk-rock Sr-Nd, clinopyroxene Sr, and zircon O isotopes demonstrate their isotopically enriched character. Combined with precollisional basalts, we suggest that the mantle source of the enclaves was enriched by the subducted Indian continent. This study implies that the Indian continent had subducted beneath central Lhasa no later than early Miocene.

Plain Language Summary India-Eurasia plate convergence has been one of the most important Cenozoic geological events on Earth. The Indian continent should now lie beneath central Lhasa block of southern Tibet, as the geophysical data showed. However, we cannot actually determine when the Indian continent reached its present position. The Cenozoic mantle-derived ultrapotassic rocks in central Lhasa, characterized by extremely enriched isotopic compositions, have often been used in attempts to trace mantle metasomatism and the geodynamic processes associated with Indian continental subduction. However, these rocks were likely contaminated by Lhasa ancient crustal materials. Uncertainties on primary ultrapotassic magmas and their origins have limited our ability to directly characterize their mantle sources. We have recently identified the early Miocene mafic enclaves in central Lhasa. Our study indicates that these enclaves likely originated in basic ultrapotassic magmas. The bulk-rock Sr-Nd, in situ clinopyroxene Sr, and zircon O isotope compositions differ from those of precollisional basalts, further demonstrating the isotopically enriched character of the primary magmas and suggesting that their mantle source was metasomatized by the subducted Indian continent. This study shows that the Indian continent could likely have reached its present position (central Lhasa block) no later than the early Miocene.

1. Introduction

India-Eurasia plate convergence has been one of the most important Cenozoic geological events on Earth. Geophysical data demonstrate that the Indian continent has subducted northward beneath southern Tibet (Gao et al., 2016; Nabělek et al., 2009; Tapponnier et al., 2001; Zhao et al., 2010), but the detailed history of Indian continental subduction remains unclear. Based on studies of ca. 14 Ma adakitic rocks in the southern Lhasa block, Xu et al. (2010) suggested that the Indian continental crust had subducted beneath southern Tibet by that time. Jiang et al. (2011, 2014) and Hou et al. (2012) interpreted the ca. 30 Ma adakitic rocks in southern Lhasa to be produced by partial melting of northward subducted lower Indian crust and suggested that the Indian continent had entered beneath southern Tibet by least 30 Ma. Recently, Ma et al. (2017) suggested that the ca. 35 Ma Quguosha gabbros in southern Lhasa had a mantle source that

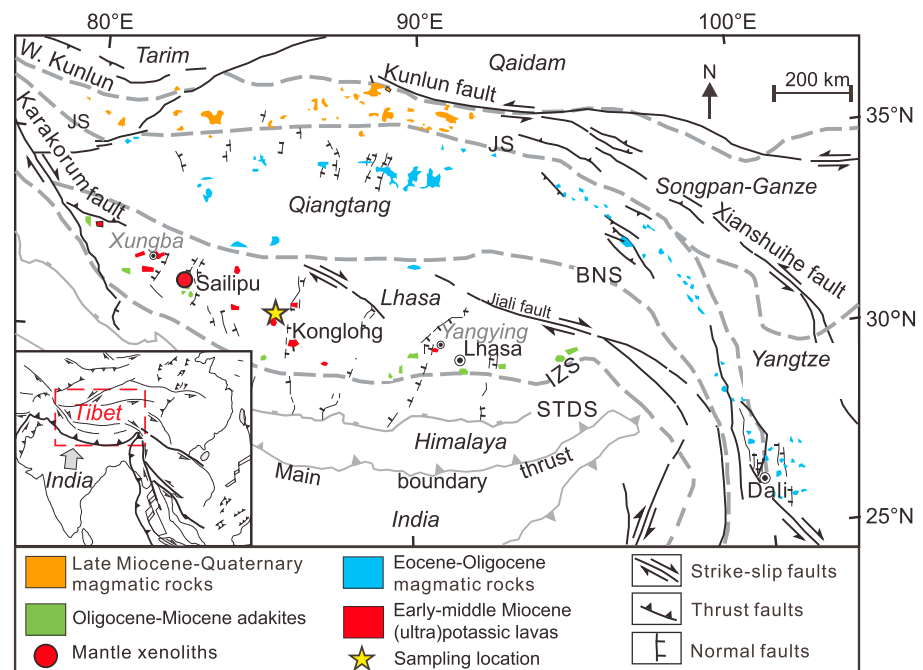


Figure 1. Sketch map of main tectonic units and distribution of Cenozoic (ultra) potassic rocks and adakites in Tibetan Plateau, modified after Yin and Harrison (2000) and Liu et al. (2011). Inset shows location of Tibet in regional context. Our mafic enclave samples are from the Konglong area in the central Lhasa block. STDS: South Tibet detachment system; IZS: Indo-Zangpo suture; BNS: Bangong-Nujiang suture; JS: Jinsha suture.

was enriched by the subducted Indian continental materials, which may imply initial continental subduction beneath southern Tibet by least 35 Ma. However, Nabélek et al. (2009), based on the geophysical data, suggested that the northern extent of the Indian crust should now lie beneath the central Lhasa block of southern Tibet. So far, we cannot actually determine when the Indian continent reached its present position beneath southern Tibet.

Cenozoic ultrapotassic rocks mainly in the central Lhasa block of southern Tibet not only provide a postcollisional window into the thermal and compositional characteristics of the deep mantle (Chung et al., 1998; Nomade et al., 2004; Turner et al., 1993; Williams et al., 2001, 2004; Xu et al., 2017); their extremely enriched isotopic compositions have also been widely used as tracers of mantle metasomatism attributed to either Tethys oceanic or Indian continental subduction (Ding et al., 2003; Gao et al., 2007; Guo et al., 2013, 2015; Zhao et al., 2009). In the latter model, the ultrapotassic rocks may record significant information relating to the past subduction of the Indian continent.

The Cenozoic ultrapotassic rocks are dominated by trachyandesites. Only minor basaltic samples have been reported (e.g., Williams et al., 2001), and these may be ascribed to the presence of olivine xenocrysts (Guo et al., 2015; Zhao et al., 2009). The genesis of the ultrapotassic lavas has been highly controversial. Some studies suggest that the ultrapotassic lavas originated directly from an enriched mantle source (Guo et al., 2015; Huang et al., 2015; Turner et al., 1996). However, other studies of crustal xenoliths, zircon xenocrysts, and bulk-rock Os isotopes (Liu et al., 2015; Liu, Zhao, Zhu, Niu, Depaolo, et al., 2014a; Liu, Zhao, Zhu, Niu, & Harrison, 2014b; Miller et al., 1999) have suggested that the ultrapotassic lavas were contaminated by ancient crust material of the Lhasa block, which would limit our ability to directly characterize the isotopic characteristics of their mantle sources.

It has been proposed that phlogopite- and spinel-bearing harzburgite mantle xenoliths entrained by ultrapotassic trachyandesites from the Sailipu area, southern Tibet, correspond to the mantle source rocks of the ultrapotassic lavas (Liu et al., 2011), implying that their mantle source can be characterized directly. Compared to the ultrapotassic lavas, however, model melts in equilibrium with the Sailipu mantle xenoliths have similar light rare earth element (LREE) and middle REE but distinctly higher heavy REE

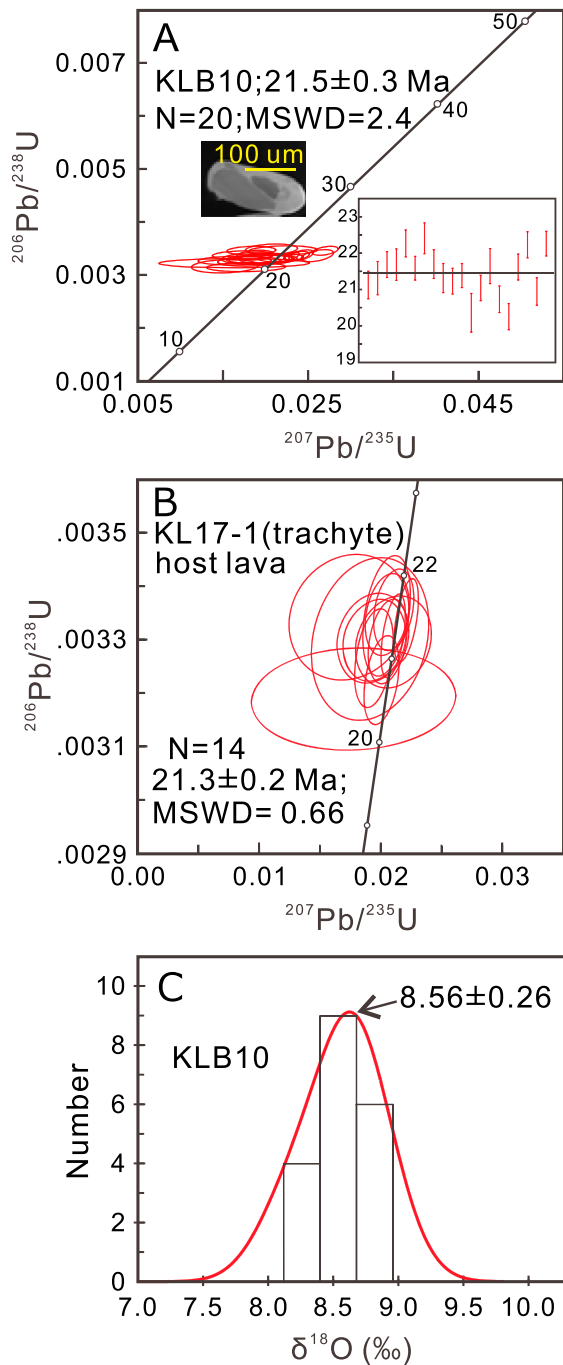


Figure 2. Secondary ion mass spectroscopy zircon U-Pb dating results for (a) the Konglong mafic enclave and (b) the host trachyte. (c) Zircon O isotopes for the mafic enclave. Representative zircons of the mafic enclave exhibit sector zoning in cathodoluminescence images. The zircons observed in the photomicrographs of the dated enclave KLB10 (Figure DR3) include examples embedded within Cpx, which can suggest their crystallization directly from the enclave magma.

(HREE) contents (Liu et al., 2011). This discrepancy suggests that the ultrapotassic lavas were not derived from the enriched lithospheric mantle represented by the Sailipu mantle xenoliths, and thus, their mantle source remains unknown.

Uncertainties regarding the primary ultrapotassic magmas and their mantle origins not only hinder attempts to establish the isotopic characteristics of their mantle sources but also obscure the mechanism of mantle metasomatism. We have recently identified mafic enclaves entrained by Miocene potassic lavas in the central Lhasa block of southern Tibet that may resolve these issues. Our study suggests that the mafic enclaves likely originated in basic ultrapotassic magmas. Accordingly, they provide an unprecedented opportunity to investigate Cenozoic primary ultrapotassic magmas and their mantle characteristics.

2. Geological Setting and Samples

The Tibetan Plateau consists primarily of the Songpan-Ganze, Qiangtang, Lhasa and Himalaya blocks, separated from north to south by the Jinsha, Bangong-Nujiang, and Indo-Zangpo suture zones (Figure 1; Yin & Harrison, 2000). The Lhasa block can be further divided into three parts (i.e., northern, central, and southern Lhasa blocks; Zhu et al., 2011; Zhu et al., 2013). The initial India-Eurasia (India-Lhasa) collision is generally suggested to have occurred in the early Cenozoic (65–55 Ma; e.g., Hu et al., 2015). The ongoing collision, where the Indian continental lithosphere is dragged by the subducted Neo-Tethyan oceanic lithosphere, would induce slab break-off (i.e., separation of the oceanic and continental lithosphere) due to the buoyancy of Indian continental lithosphere (Zhu et al., 2015). The slab break-off most likely occurred at 50–45 Ma, based on a magmatic flare-up and the presence of ocean island basalt-type rocks (Ji et al., 2016; Jiang et al., 2014; Zhu et al., 2015). After slab break-off, the collision zone converted into an intracontinental setting with the convergence of the Indian continental lithosphere beneath southern Tibet. The initial subduction of the Indian continent likely occurred at 35 Ma (Ma et al., 2017). As previously noted, the present northern extent of the Indian continent beneath the central Lhasa block is shown by geophysical data (Nabělek et al., 2009), but the time at which the Indian continental plate first reached its present position remains unclear.

Cenozoic postcollisional volcanic rocks in the central Lhasa block of southern Tibet mainly consist of 24–8 Ma potassic-ultrapotassic lavas (Figure 1; Miller et al., 1999; Turner et al., 1996). The ultrapotassic lavas commonly crop out west of longitude 87°E, and rare samples occur at longitude 90°E (Xu et al., 2017), whereas potassic lavas are sporadically distributed in the Xungba, Konglong, and Yangying areas (Figure 1; Miller et al., 1999; Nomade et al., 2004).

The postcollisional volcanic rocks in the Konglong area of central Lhasa are composed of trachytes with minor rhyolites and erupted at 21.3 ± 0.2 Ma (a whole-rock ^{40}Ar - ^{39}Ar age of a rhyolite; Chen et al., 2010). Mafic enclaves entrained in the trachytes consist principally of clinopyroxene, phlogopite, and K-feldspar and accessory apatite, sphene, and zircon (Figure DR2). Detailed petrographic, geochronological, mineral, and bulk-rock geochemical analyses were conducted on the Konglong enclaves.

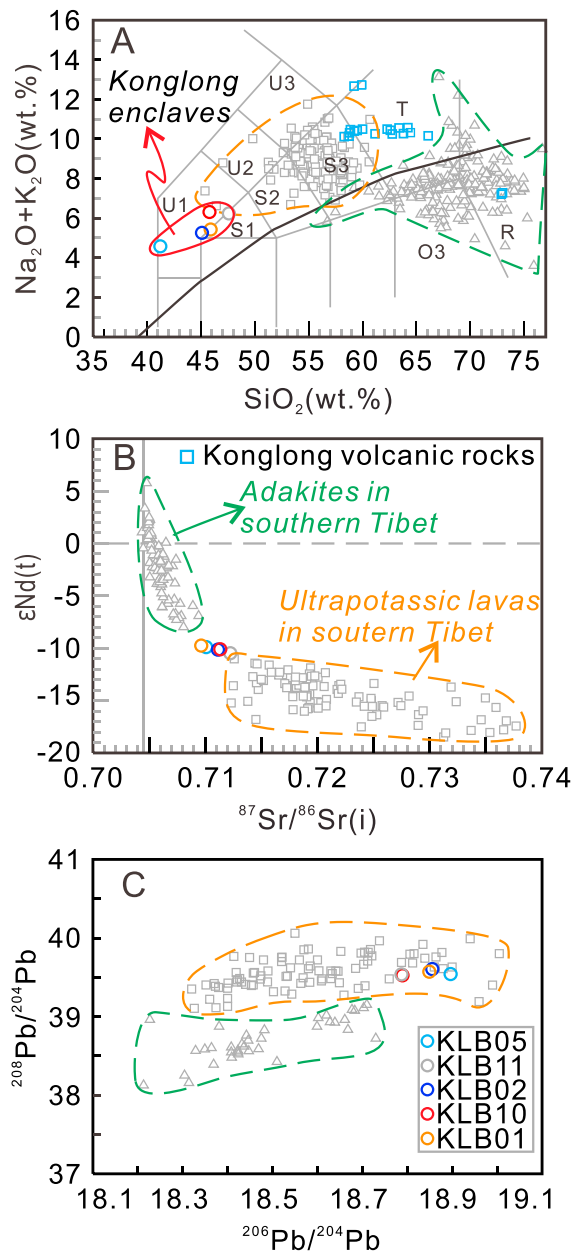


Figure 3. (a) Total alkali versus SiO₂ and (b) Sr-Nd isotopes and (c) Pb isotopes of the Konglong mafic enclaves. The Konglong volcanic rock data are from Chen et al. (2010). The postcollisional ultrapotassic lavas and adakites in southern Tibet (data sources are the same as in Figure DR4) are for comparison. O3-dacite; R-rhyolite; S1-trachybasalt; S2-basaltic trachyandesite; S3-trachyandesite; T-trachyte; U2-phonotephrite; U3-tephriphonolite.

However, numerous studies (e.g., Guo et al., 2015; Williams et al., 2001) have indicated that they commonly have SiO₂ of 52–61 wt % (i.e., trachyandesites rather than basalts; Figure 3a), MgO of 5–10 wt %, and extremely enriched Sr-Nd isotope compositions (⁸⁷Sr/⁸⁶Sr(i) > 0.712, εNd(t) < –11.0; Figure 3b). It should be noted that basalt outcrops are comparatively rare and only a few lava samples are basaltic (four samples have SiO₂ of 45–50 wt %; Figure 3a) and have relatively high MgO (>10 wt %). These exceptional samples may be ascribed to the presence of the mantle olivine xenocrysts in the ultrapotassic lavas (e.g., Guo et al., 2015; Liu et al., 2011; Zhao et al., 2009).

3. Results

Secondary ion mass spectroscopy zircon U-Pb dating for the Konglong mafic enclaves yields a weighted mean ²⁰⁶Pb/²³⁸U age of 21.5 ± 0.3 Ma, similar to that of the trachyte host lavas (21.3 ± 0.2 Ma; Figures 2a and 2b). Zircons in the mafic enclaves show limited δ¹⁸O ranges of 8.1–8.9‰ with an average value of 8.56 ± 0.26‰ (1SD; Figure 2c).

The Konglong mafic enclaves have high MgO (8.9–11.1 wt %) and K₂O contents (3.8–5.4 wt %) and K₂O/Na₂O ratios (4.0–6.0) and thus are ultrapotassic (Foley et al., 1987) but are distinguished from the ultrapotassic lavas (i.e., trachyandesites) in southern Tibet by their lower SiO₂ (41.2–47.6 wt %, volatile-free; Figure 3a). They are characterized by relatively flat LREE patterns, HREE depletions, moderate negative Eu anomalies and significant enrichment of the large ion lithophile elements relative to the high field strength elements (Figures DR4a and DR4b). The trace element distribution patterns of the Konglong enclaves closely resemble those of the ultrapotassic lavas but clearly differ from those of the postcollisional adakitic intrusions in southern Tibet (Figures DR4a and DR4b). The enclaves have highly enriched Sr-Nd isotopic compositions (⁸⁷Sr/⁸⁶Sr(i) = 0.710 to 0.712 and εNd(t) = –9.8 to –10.5), close to but slightly less enriched than those (⁸⁷Sr/⁸⁶Sr(i) > 0.712, εNd(t) < –11.0) of the ultrapotassic lavas (Figure 3b). They also have high Pb isotopic ratios, similar to those of the ultrapotassic lavas but unlike those of the adakites (Figure 3c).

Phlogopites (Phl) in the Konglong enclaves have variable Mg# of 37–84 and K₂O and Al₂O₃ contents of 6.2–11.2 and 9.0–14.0 wt %, respectively, distinct from those of Phl in the Sailipu mantle xenoliths but similar to those of Phl phenocrysts in the Sailipu ultrapotassic lavas (Figures DR5a and DR5b). Feldspars have high K₂O contents and are sanidine (Figure DR5c). Clinopyroxenes (Cpx) have variable Mg# of 63–89 and high CaO contents of 21.7–24.7 wt % (Figure 4a) and are diopside and sahlite, in contrast to the high Mg# (84–89) and low CaO (18.4–21.6 wt %) of the endiopsides in the Sailipu mantle xenoliths (Figure DR5d). Clinopyroxenes display upward-convex REE patterns with small negative Eu anomalies (Figure DR4c). Compared to Cpx in the Sailipu mantle xenoliths (Liu et al., 2011), the high Mg# (84–89) clinopyroxenes in the Konglong enclaves generally have lower trace element contents, except for Sr (Figure 4b). The clinopyroxenes in the enclaves commonly have homogeneous and lower Sr isotope values (0.709–0.714), except for several grains with ⁸⁷Sr/⁸⁶Sr of 0.715–0.716 (Figure 4c), whereas clinopyroxenes in the Sailipu xenoliths have high Sr isotope ratios (0.714–0.719; Xu et al., 2017).

4. Discussions

4.1. Primary Ultrapotassic Magmas

Miocene ultrapotassic lavas (e.g., MgO > 3 wt %, K₂O > 3 wt %, K₂O/Na₂O > 2; Foley et al., 1987) are widely distributed in southern Tibet.

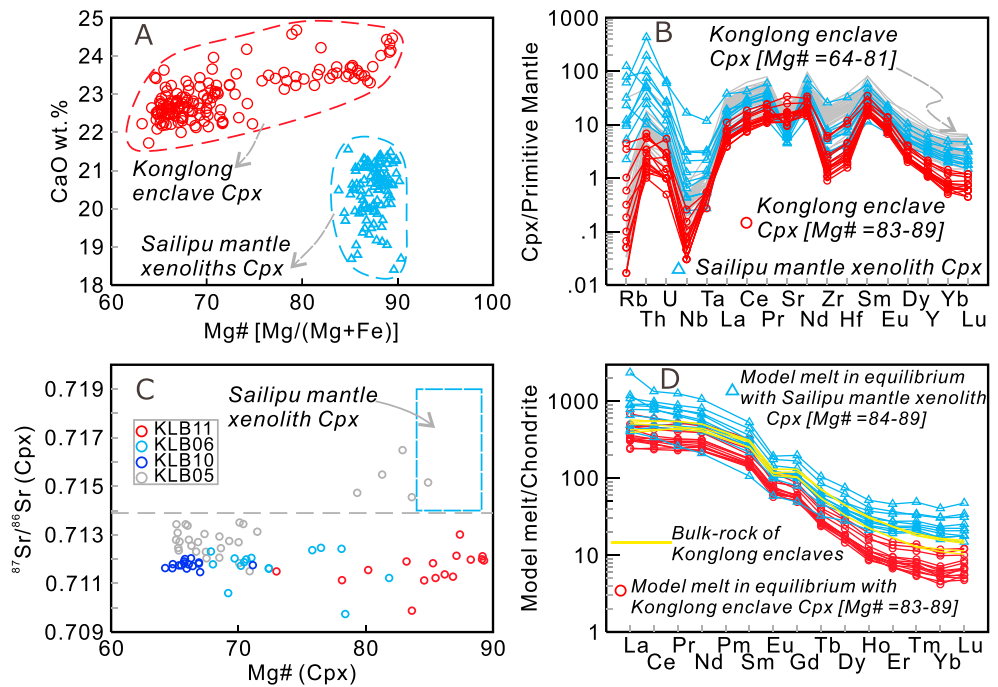


Figure 4. (a) CaO versus Mg# of the Konglong enclave Cpx. (b) Trace element contents of Cpx from Konglong enclaves normalized to primitive mantle. (c) In situ Sr isotopes versus Mg# of the Konglong enclave Cpx. Individual errors are smaller than the size of the symbols used. (d) Rare earth element compositions of model melts in equilibrium with the Konglong enclave Cpx normalized to chondrite. Normalizing values are from Sun and McDonough (1989). The major, trace elemental data and in situ Sr isotopes for Cpx of the Sailipu mantle xenoliths are from Liu et al. (2011) and Xu et al. (2017), respectively.

The Konglong mafic enclaves are contemporary with the postcollisional ultrapotassic (trachyandesite) lavas in southern Tibet. Compared to the ultrapotassic lavas, the Konglong mafic enclaves show similar REE distribution patterns and spider diagrams, but lower SiO₂ (41–48 wt %), higher MgO (9–11 wt %), and less enriched Sr–Nd isotopes ($^{87}\text{Sr}/^{86}\text{Sr}(i) = 0.710\text{--}0.712$, $\epsilon\text{Nd}(t) = -9.8$ to -10.5 ; Figure 3). Moreover, the compositions of the minerals in the mafic enclaves show clearly that they are phenocrysts rather than xenocrysts. Thus, the combination of their high K₂O, K₂O/Na₂O, and mineral assemblage (Cpx + Phl + sanidine) demonstrates that the mafic enclaves are primary/basic ultrapotassic rocks, which are unique in southern Tibet and reported here for the first time. Their primary/basic nature is also consistent with the high Mg# (up to 89) of the clinopyroxenes in the enclaves. The calculated Mg# of the parental liquids in equilibrium with the clinopyroxenes, using the method of Wood and Blundy (1997), extends up to 70, coinciding with those of mantle-derived primary melts. Based on this evidence, the Konglong mafic enclaves must have originated from primary ultrapotassic magmas.

Early crystallizing minerals (e.g., high Mg# clinopyroxenes) instead of the whole rock typically record more direct information regarding primary magma compositions and their source regions (Ren et al., 2017). We calculated REE compositions of the model melts in equilibrium with the enclave clinopyroxenes with Mg# of 83–89, using partition coefficients between Cpx and an alkaline lamprophyric melt from Foley et al. (1996). The model melts (Figure 4d) have flat LREE patterns and a more significant HREE fractionation than spinel mantle-derived melts (Liu et al., 2011), indicating a garnet-facies mantle source for the primary magmas. Moreover, the primary ultrapotassic magmas were isotopically enriched, as demonstrated by the in situ clinopyroxene Sr and zircon O isotopic compositions of the Konglong enclaves.

4.2. Formation of Mafic Enclaves

Although the Konglong mafic enclaves originated from primary magmas, they may have experienced complex magma chamber processes (e.g., mixing of variable magmas, AFC, and accumulation). Indeed, a noticeable discrepancy of REE contents occurs between the enclaves and model primary magmas, indicating that the primary magma assimilated/mixed with other high-REE components to form the enclaves. The majority

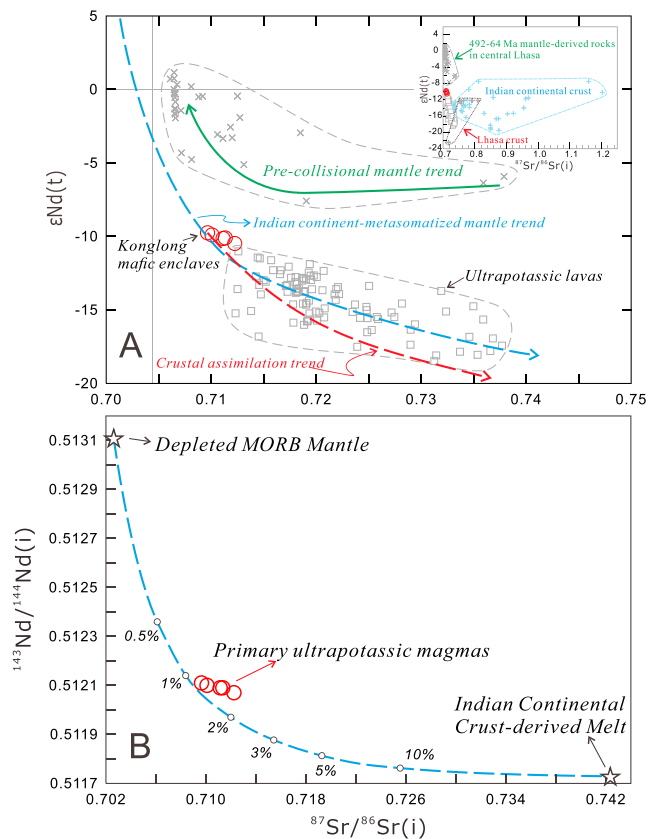


Figure 5. (a) Sr-Nd isotope diagram. The green line shows the isotopic trend of the oceanic subduction-related mantle from 492 to 64 Ma. Isotopic compositions of 492–64 Ma mantle-derived rocks in central Lhasa are from Zhu et al. (2010, 2012), Chen et al. (2014), Meng et al. (2014), and Qi et al. (2018). The red line shows that the primary ultrapotassic magmas with less enriched isotope compositions are parental to the ultrapotassic lavas and can produce the ultrapotassic lavas by Lhasa crustal contamination. The Lhasa crustal Sr-Nd isotopic compositions are from Zhu et al. (2012) and Miller et al. (1999). The blue line shows that primary ultrapotassic magmas most plausibly originated from a depleted mantle source that was metasomatized by the subducted Indian continental crust. The Indian continental crustal isotopic components are based on those of the Himalayan metapelites, gneisses, and Miocene leucogranites (Zeng et al., 2011). (b) Simple mixing modeling shows that the mantle source of primary ultrapotassic magmas can be a hybrid mantle consisting of the depleted mantle and 1–2% melts derived from the Indian continental crust. The selected end-members are discussed in the text, and their isotope compositions (crustal melt: Sr = 141.28 ppm, ⁸⁷Sr/⁸⁶Sr_i = 0.742355; Nd = 45.45 ppm, ¹⁴³Nd/¹⁴⁴Nd_(i) = 0.511725; depleted mantle: Sr = 7.664 ppm, ⁸⁷Sr/⁸⁶Sr_i = 0.702626; Nd = 0.581 ppm, ¹⁴³Nd/¹⁴⁴Nd_(i) = 0.513106) are from Guo et al. (2013).

of clinopyroxenes in the Konglong enclaves and those in the Sailipu mantle xenoliths have distinct Sr isotopic compositions (Figure 4c), suggesting that the spinel mantle was not involved substantially in the formation of the enclaves. This could be ascribed to a rapid ascent of the garnet-facies mantle-derived primary magmas to the crust (Figure DR6). The similar Sr isotopic compositions of the Konglong enclaves and their clinopyroxenes imply only limited crustal assimilation during their formation. Instead, the most plausible contaminant is differentiated products of the primary magmas themselves. Therefore, we suggest that mixing of garnet mantle-derived primary magmas and their differentiated derivatives (self-mixing, Couch et al., 2001; Figure DR6) can readily explain the genesis of the enclaves.

4.3. Petrogenetic and Geodynamic Implications

The question of whether Miocene ultrapotassic lavas in southern Tibet have been significantly contaminated by Lhasa ancient crust remains controversial. Some studies (e.g., Zhao et al., 2009) argued against crustal assimilation, mainly based on the fact that the lower trace elemental contents of the continental crust would dilute those of the ultrapotassic lavas. In this genetic model, the variable geochemical compositions of the ultrapotassic rocks (including the lavas and mafic enclaves) were considered to have resulted from the heterogeneity of the mantle source. However, numerous crustal xenoliths and zircon xenocrysts found in the ultrapotassic lavas may indicate significant crustal assimilation (Liu, Zhao, Zhu, Niu, Depaolo, et al., 2014a; Liu, Zhao, Zhu, Niu, & Harrison, 2014b; Miller et al., 1999). This scenario is consistent with the variably high ¹⁸⁷Os/¹⁸⁸Os values of the ultrapotassic lavas that were most likely caused by crustal assimilation (Liu et al., 2015). Given that the Konglong mafic enclaves likely originated from primary ultrapotassic magmas, they can provide key petrogenetic information concerning the origin and evolution of these magmas. Compared to the enclaves, for example, the trachyandesites show more enriched Sr-Nd isotopic compositions (Figure 5), which support a role for Lhasa crust assimilation during their generation. Importantly, the majority of the ultrapotassic lavas are localized in the central Lhasa block, which indeed has an isotopically enriched ancient basement (Figure 5; Zhu et al., 2011; Zhu et al., 2013).

The ultrapotassic lavas in southern Tibet are characterized by extremely enriched isotopic compositions, which have widely been ascribed to an enriched mantle source metasomatized by subducted Tethyan oceanic sediments (e.g., Gao et al., 2007) or Indian continental crust (Ding et al., 2003; Guo et al., 2015). In order to identify the agent for mantle metasomatism, the following issues are addressed sequentially: (1) the isotopic nature of the metasomatized mantle, (2) the mantle's evolution and composition prior to metasomatism, and (3) the subducted components contributing to mantle metasomatism. As noted above, crustal contamination in the ultrapotassic lavas of southern Tibet has limited our ability to directly characterize their mantle sources. With the recognition of the mafic enclaves, however, primary magma characteristics can now be used to define effectively the source and to resolve their geodynamic context.

We have combined our new isotopic results with previously reported data for ~492–64 Ma mafic rocks of the central Lhasa block to characterize the isotopic evolutionary trend of the local mantle (Figure 5a). The ancient enriched mantle was gradually replaced by relatively less enriched to slightly depleted mantle from the Cambrian (492 Ma) to the early Cenozoic (64 Ma). Such evolving characteristics were most likely caused by long-term (Paleo-Tethyan, Songdo, Bangong-Nujiang, and Neo-Tethyan) oceanic subduction (Zhu et al.,

2013), which would have introduced isotopically depleted components (e.g., basaltic oceanic crust-derived melts or fluids) into the mantle. The slightly depleted mantle that was present at 64 Ma was transformed into an enriched mantle by 21 Ma, as indicated by the Konglong enclaves. We suggest that such a shift may be induced by Indian continental subduction, based on the following evidence: (1) The mantle evolutionary trend shows that long-term oceanic subduction beneath central Lhasa introduced significantly depleted rather than enriched components into the mantle; (2) the Neo-Tethyan oceanic slab had likely been detached from the orogenic system and moved into the deep mantle by 45 Ma (Chung et al., 2005), and the Indian continent has begun to subduct beneath southern Tibet at 35 Ma (Ma et al., 2017); and (3) the Indian continental crust has extremely enriched Sr-Nd-O isotopic components (Figure 5a). A simple Sr-Nd isotope mixing modeling is used to illustrate the effect of mantle metasomatism by the Indian continental crust (Figure 5b). A melt derived from the biotite gneiss within the Greater Himalayan Sequence was taken as the enriched end-member, and its isotopic compositions ($\text{Sr} = 141.28 \text{ ppm}$, $^{87}\text{Sr}/^{86}\text{Sr}_{(i)} = 0.742355$; $\text{Nd} = 45.45 \text{ ppm}$, $^{143}\text{Nd}/^{144}\text{Nd}_{(i)} = 0.511725$) are from Guo et al. (2013). The other end-member can likely be represented by the depleted MORB mantle (DMM; Guo et al., 2013). The following factors were likely important in establishing how mixing proceeded: (1) The mantle affected by the oceanic subduction tended to be a hydrous and softened mantle and therefore was susceptible to shortening and thickening by the northward impingement of the Indian continent between 45 and 35 Ma (Chung et al., 2005); (2) subsequent delamination of this thickened mantle would create space and promote the initial subduction of the Indian continent at 35 Ma; (3) as a result of the delamination, the subducted Indian continental plate was likely to metasomatize newly introduced DMM. Mixing model results show that the enriched mantle source of the Konglong enclaves can be a hybrid mantle consisting of the DMM and 1–2% melts derived from the Indian continental crust. Notably, the Konglong enclaves have high zircon $\delta^{18}\text{O}$ values of 8.1–8.9‰ within the range of those of the Greater Himalayan Sequence and its leucogranites (6.9–12.5‰; Hopkinson et al., 2017), further arguing for a mantle source metasomatized by the Indian continental crust.

Collectively, this new evidence implies that the Indian continent had subducted beneath the central Lhasa block no later than the early Miocene. If the present northernmost position of the Indian continent beneath southern Tibet determined by Nabělek et al. (2009) is accurate, then our evidence suggests that the Indian continent has reached this position no later than the early Miocene.

Acknowledgments

We thank the Editor Professor Jeroen Ritsema and two reviewers for their constructive comments which significantly improved our paper. The data supporting the conclusions can be found in the Supporting Information. Financial support for this research was provided by the National Natural Science Foundation of China (41630208), the Key Program of the Chinese Academy of Sciences (QYZDJ-SSW-DQC026), the National Key R & D Program of China (2016YFC0600407), and the Key Science Program of Guangzhou City (201707020032), the Guangzhou Institute of Geochemistry, Chinese Academy of Sciences (GIGCAS 135 Project [135TP201601]) and the China Postdoctoral Science Foundation funded project (grant 2017M620263). This is contribution IS-2570 from GIGCAS.

References

- Chen, J. L., Xu, J. F., Wang, B. D., Kang, Z. Q., & Li, J. (2010). Origin of Cenozoic alkaline potassic volcanic rocks at KonglongXiang, Lhasa terrane, Tibetan Plateau: Products of partial melting of a mafic lower-crustal source? *Chemical Geology*, 273(3-4), 286–299. <https://doi.org/10.1016/j.chemgeo.2010.03.003>
- Chen, Y., Zhu, D., Zhao, Z., Meng, F., Wang, Q., Santosh, M., et al. (2014). Slab breakoff triggered ca. 113 Ma magmatism around Xainza area of the Lhasa Terrane. *Tibet. Gondwana Res*, 26(2), 449–463. <https://doi.org/10.1016/j.jgr.2013.06.005>
- Chung, S. L., Chu, M.-F., Zhang, Y., Xie, Y., Lo, C.-H., Lee, T.-Y., et al. (2005). Tibetan tectonic evolution inferred from spatial and temporal variations in post-collisional magmatism. *Earth Science Reviews*, 68(3-4), 173–196. <https://doi.org/10.1016/j.earscirev.2004.05.001>
- Chung, S.-L., Lo, C.-H., Lee, T.-Y., Zhang, Y., Xie, Y., Li, X., et al. (1998). Diachronous uplift of the Tibetan Plateau starting 40 Myr ago. *Nature*, 394(6695), 769–773. <https://doi.org/10.1038/29511>
- Couch, S., Sparks, R. S., & Carroll, M. R. (2001). Mineral disequilibrium in lavas explained by convective self-mixing in open magma chambers. *Nature*, 411(6841), 1037–1039. <https://doi.org/10.1038/35082540>
- Ding, L., Kapp, P., Zhong, D. L., & Deng, W. M. (2003). Cenozoic volcanism in Tibet: Evidence for a transition from oceanic to continental subduction. *Journal of Petrology*, 44(10), 1833–1865. <https://doi.org/10.1093/ptrology/egg061>
- Foley, S. F., Jackson, S. E., Fryer, B. J., Greenough, J. D., & Jenner, G. A. (1996). Trace element partition coefficients for clinopyroxene and phlogopite in an alkaline lamprophyre from Newfoundland by LAM-ICP-MS. *Geochim Cosmochim Acta*, 60(4), 629–638. [https://doi.org/10.1016/0016-7037\(95\)00422-X](https://doi.org/10.1016/0016-7037(95)00422-X)
- Foley, S. F., Venturelli, G., Green, D. H., & Toscani, L. (1987). The ultrapotassic rocks: Characteristics, classification, and constraints for petrogenetic models. *Earth Science Reviews*, 24(2), 81–134. [https://doi.org/10.1016/0012-8252\(87\)90001-8](https://doi.org/10.1016/0012-8252(87)90001-8)
- Gao, R., Lu, Z., Klempner, S., Wang, H., Dong, S., Li, W., & Li, H. (2016). Crustal-scale duplexing beneath the Yarlung Zangbo suture in the western Himalaya. *Nature Geoscience*, 9(7), 555–560. <https://doi.org/10.1038/ngeo2730>
- Gao, Y., Hou, Z., Kamber, B. S., Wei, R., Meng, X., & Zhao, R. (2007). Lamproitic rocks from a continental collision zone: Evidence for recycling of subducted Tethyan oceanic sediments in the mantle beneath southern Tibet. *Journal of Petrology*, 48(4), 729–752. <https://doi.org/10.1093/ptrology/egl080>
- Guo, Z. F., Wilson, M., Zhang, M., Cheng, Z., & Zhang, L. (2015). Post-collisional ultrapotassic mafic magmatism in South Tibet: Products of partial melting of pyroxenite in the mantle wedge induced by roll-back and delamination of the subducted Indian continental lithosphere slab. *Journal of Petrology*, 56(7), 1365–1406. <https://doi.org/10.1093/ptrology/egv040>
- Guo, Z. F., Wilson, M., Zhang, M. L., Cheng, Z. H., & Zhang, L. H. (2013). Post-collisional, K-rich mafic magmatism in South Tibet: Constraints on Indian slab-to-wedge transport processes and plateau uplift. *Contrib Mineral Petr*, 165(6), 1311–1340. <https://doi.org/10.1007/s00410-013-0860-y>

- Hopkinson, T., Harris, N., Warren, C., Spencer, C., Roberts, N., Horstwood, M., et al. (2017). The identification and significance of pure sediment-derived granites. *Earth and Planetary Science Letters*, *467*, 57–63. <https://doi.org/10.1016/j.epsl.2017.03.018>
- Hou, Z. Q., Zheng, Y. C., Zeng, L. S., Gao, L. E., Huang, K. X., Li, W., et al. (2012). Eocene-Oligocene granitoids in southern Tibet: Constraints on crustal anatexis and tectonic evolution of the Himalayan orogen. *Earth and Planetary Science Letters*, *349–350*, 38–52. <https://doi.org/10.1016/j.epsl.2012.06.030>
- Hu, X., Garzanti, E., Moore, T., & Raffi, I. (2015). Direct stratigraphic dating of India-Asia collision onset at the Selandian (middle Paleocene, 59±1 Ma). *Geology*, *43*(10), 859–862. <https://doi.org/10.1130/G36872.1>
- Huang, F., Chen, J., Xu, J., Wang, B., & Li, J. (2015). Os-Nd-Sr isotopes in Miocene ultrapotassic rocks of southern Tibet: Partial melting of a pyroxenite-bearing lithospheric mantle? *Geochim Cosmochim Acta*, *163*, 279–298. <https://doi.org/10.1016/j.gca.2015.04.053>
- Ji, W. Q., Wu, F. Y., Chung, S. L., Wang, X. C., Liu, C. Z., Li, Q. L., et al. (2016). Eocene neo-Tethyan slab breakoff constrained by 45 Ma oceanic island basalt-type magmatism in southern Tibet. *Geology*, *44*(4), 283–286. <https://doi.org/10.1130/G37612.1>
- Jiang, Z. Q., Wang, Q., Wyman, D. A., Li, Z. X., Yang, J. H., Shi, X. B., et al. (2014). Transition from oceanic to continental lithosphere subduction in southern Tibet: Evidence from the Late Cretaceous-Early Oligocene (~91–30 Ma) intrusive rocks in the Chanang-Zedong area, southern Gangdese. *Lithos*, *196–197*, 213–231. <https://doi.org/10.1016/j.lithos.2014.03.001>
- Jiang, Z. Q., Wang, Q., Wyman, D. A., Tang, G. J., Jia, X. H., Yang, Y. H., & Yu, H. X. (2011). Origin of ~30Ma Chongmuda adakitic intrusive rocks in the southern Gangdese region, southern Tibet: Partial melting of the northward subducted Indian continent crust? *Geochimica*, *40*, 126–146.
- Liu, C. Z., Wu, F. Y., Chung, S. L., & Zhao, Z. D. (2011). Fragments of hot and metasomatized mantle lithosphere in Middle Miocene ultrapotassic lavas, southern Tibet. *Geology*, *39*(10), 923–926. <https://doi.org/10.1130/G32172.1>
- Liu, D., Zhao, Z., Zhu, D., Niu, Y., Depaolo, D. J., Harrison, T. M., et al. (2014a). Postcollisional potassic and ultrapotassic rocks in southern Tibet: Mantle and crustal origins in response to India-Asia collision and convergence. *Geochim Cosmochim Acta*, *143*, 207–231. <https://doi.org/10.1016/j.gca.2014.03.031>
- Liu, D., Zhao, Z., Zhu, D., Niu, Y., & Harrison, T. M. (2014b). Zircon xenocrysts in Tibetan ultrapotassic magmas: Imaging the deep crust through time. *Geology*, *42*(1), 43–46. <https://doi.org/10.1130/G34902.1>
- Liu, D., Zhao, Z., Zhu, D., Niu, Y., Widom, E., Teng, F., et al. (2015). Identifying mantle carbonatite metasomatism through Os-Sr-Mg isotopes in Tibetan ultrapotassic rocks. *Earth and Planetary Science Letters*, *458–469*.
- Ma, L., Wang, Q., Li, Z.-X., Wyman, D. A., Yang, J.-H., Jiang, Z.-Q., et al. (2017). Subduction of Indian continent beneath southern Tibet in the latest Eocene (~35 Ma): Insights from the Quguosha gabbros in southern Lhasa block. *Gongwana Res*, *41*, 77–92. <https://doi.org/10.1016/j.gr.2016.02.005>
- Meng, F., Zhao, Z., Zhu, D., Mo, X., Guan, Q., Huang, Y., et al. (2014). Late Cretaceous magmatism in Mamba area, Central Lhasa subterrane: Products of back-arc extension of neo-Tethyan Ocean? *Gondwana Research*, *26*(2), 505–520. <https://doi.org/10.1016/j.gr.2013.07.017>
- Miller, C., Schuster, R., Klotzli, U., Frank, W., & Purtscheller, F. (1999). Post-collisional potassic and ultrapotassic magmatism in SW Tibet: Geochemical and Sr-Nd-Pb-O isotopic constraints for mantle source characteristics and petrogenesis. *Journal of Petrology*, *40*(9), 1399–1424. <https://doi.org/10.1093/ptro/40.9.1399>
- Nabělek, J., Hetenyi, G., Vergne, J., Sapkota, S. N., Kafle, B., Jiang, M., et al. (2009). Underplating in the Himalaya-Tibet collision zone revealed by the hi-CLIMB experiment. *Science*, *325*(5946), 1371–1374. <https://doi.org/10.1126/science.1167719>
- Nomade, S., Renne, P. R., Mo, X., Zhao, Z., & Zhou, S. (2004). Miocene volcanism in the Lhasa block, Tibet: Spatial trends and geodynamic implications. *Earth and Planetary Science Letters*, *221*(1–4), 227–243. [https://doi.org/10.1016/S0012-821X\(04\)00072-X](https://doi.org/10.1016/S0012-821X(04)00072-X)
- Qi, Y., Gou, G. N., Wang, Q., Wyman, D. A., Jiang, Z. Q., Li, Q. L., & Zhang, L. (2018). Cenozoic mantle composition evolution of southern Tibet indicated by Paleocene (~64 Ma) pseudoleucite phonolitic rocks in Central Lhasa Terrane. *Lithos*, *302–303*, 178–188. <https://doi.org/10.1016/j.lithos.2017.12.021>
- Ren, Z.-Y., Wu, Y.-D., Zhang, L., Nichols, A. R. L., Hong, L.-B., Zhang, Y.-H., et al. (2017). Primary magmas and mantle sources of Emeishan basalts constrained from major element, trace element and Pb isotope compositions of olivine-hosted melt inclusions. *Geochim Cosmochim Acta*, *208*, 63–85. <https://doi.org/10.1016/j.gca.2017.01.054>
- Sun, S.-S., & McDonough, W. F. (1989). Chemical and isotopic systematics of oceanic basalts: Implications for mantle composition and processes. In Saunders, A.D., and Norry, M.J., eds., magmatism in the Ocean Basins. *Geological Society London Special Publications*, *42*, 313–345.
- Tapponnier, P., Xu, Z. U., Roger, F., Meyer, B., Arnaud, N., Wittlinger, G., & Yang, J. (2001). Oblique stepwise rise and growth of the Tibetan Plateau. *Science*, *294*(5547), 1671–1677. <https://doi.org/10.1126/science.105978>
- Turner, S., Arnaud, N., Liu, J., Rogers, N., Hawkesworth, C., Harris, N., et al. (1996). Post-collision, shoshonitic volcanism on the Tibetan Plateau: Implications for convective thinning of the lithosphere and the source of Ocean Island basalts. *Journal of Petrology*, *37*(1), 45–71. <https://doi.org/10.1093/ptrology/37.1.45>
- Turner, S., Hawkesworth, C., Liu, J., Rogers, N., Kelley, S., & Calsteren, P. (1993). Timing of Tibetan uplift constrained by analysis of volcanic rocks. *Nature*, *364*(6432), 50–54. <https://doi.org/10.1038/364050a0>
- Williams, H., Turner, S., Kelley, S., & Harris, N. (2001). Age and composition of dikes in southern Tibet: New constraints on the timing of east-west extension and its relationship to postcollisional volcanism. *Geology*, *29*(4), 339–342. [https://doi.org/10.1130/0091-7613\(2001\)029<0339:AACODI>2.0.CO;2](https://doi.org/10.1130/0091-7613(2001)029<0339:AACODI>2.0.CO;2)
- Williams, H. M., Turner, S., Pearce, J., Kelley, S., & Harris, N. (2004). Nature of the source regions for post-collisional, potassic magmatism in southern and northern Tibet from geochemical variations and inverse trace element modelling. *J. Petrol.*, *45*(3), 555–607.
- Wood, B. J., & Blundy, J. D. (1997). A predictive model for rare earth element partitioning between clinopyroxene and anhydrous silicate melt. *Contrib Mineral Petr*, *129*(2–3), 166–181. <https://doi.org/10.1007/s004100050330>
- Xu, B., Griffin, W. L., Xiong, Q., Hou, Z., Reilly, S. Y., Guo, Z., et al. (2017). Ultrapotassic rocks and xenoliths from South Tibet: Contrasting styles of interaction between lithospheric mantle and asthenosphere during continental collision. *Geology*, *45*(1), 51–54. <https://doi.org/10.1130/G38466.1>
- Xu, W.-C., Zhang, H.-F., Guo, L., & Yuan, H.-L. (2010). Miocene high Sr/Y magmatism, South Tibet: Product of partial melting of subducted Indian continental crust and its tectonic implication. *Lithos*, *114*(3–4), 293–306. <https://doi.org/10.1016/j.lithos.2009.09.005>
- Yin, A., & Harrison, T. M. (2000). Geologic evolution of the Himalayan-Tibetan orogen. *Annu Rev Earth Pl Sc*, *28*(1), 211–280. <https://doi.org/10.1146/annurev.earth.28.1.211>
- Zeng, L. S., Gao, L. E., Xie, K. J., & Jing, L. Z. (2011). Mid-Eocene high Sr/Y granites in the northern Himalayan gneiss domes: Melting thickened lower continental crust. *Earth and Planetary Science Letters*, *303*(3–4), 251–266. <https://doi.org/10.1016/j.epsl.2011.01.005>
- Zhao, J., Yuan, X., Liu, H., Kumar, P. P., Pei, S., Kind, R., et al. (2010). The boundary between the Indian and Asian tectonic plates below Tibet. *P Natl Acad Sci USA*, *107*(25), 11,229–11,233. <https://doi.org/10.1073/pnas.1001921107>

- Zhao, Z., Mo, X., Dilek, Y., Niu, Y., DePaolo, D., Robinson, P., et al. (2009). Geochemical and Sr-Nd-Pb-O isotopic compositions of the post-collisional ultrapotassic magmatism in SW Tibet: Petrogenesis and implications for India intra-continental subduction beneath southern Tibet. *Lithos*, *113*(1-2), 190–212. <https://doi.org/10.1016/j.lithos.2009.02.004>
- Zhu, D., Wang, Q., Zhao, Z., Chung, S., Cawood, P. A., Niu, Y., et al. (2015). Magmatic record of India-Asia collision. *Scientific Reports*, *5*(1), 14,289–14,289. <https://doi.org/10.1038/srep14289>
- Zhu, D., Zhao, Z., Niu, Y., Dilek, Y., Hou, Z., & Mo, X. (2013). The origin and pre-Cenozoic evolution of the Tibetan Plateau. *Gondwana Research*, *23*(4), 1429–1454. <https://doi.org/10.1016/j.gr.2012.02.002>
- Zhu, D. C., Mo, X. X., Zhao, Z. D., Niu, Y. L., Wang, L. Q., Chu, Q. H., et al. (2010). Presence of Permian extension- and arc-type magmatism in southern Tibet: Paleogeographic implications. *GSA Bulletin*, *122*(7-8), 979–993. <https://doi.org/10.1130/B30062.1>
- Zhu, D. C., Zhao, Z. D., Niu, Y., Mo, X. X., Chung, S. L., Hou, Z. Q., et al. (2011). The Lhasa terrane: Record of a microcontinent and its histories of drift and growth. *Earth and Planetary Science Letters*, *301*(1-2), 241–255. <https://doi.org/10.1016/j.epsl.2010.11.005>
- Zhu, D. C., Zhao, Z. D., Niu, Y. L., Dilek, Y., Wang, Q., Ji, W. H., et al. (2012). Cambrian bimodal volcanism in the Lhasa Terrane, southern Tibet: Record of an early Paleozoic Andean-type magmatic arc in the Australian proto-Tethyan margin. *Chemical Geology*, *328*, 290–308. <https://doi.org/10.1016/j.chemgeo.2011.12.024>